Tunable Injection Barrier in Organic Resistive Switches Based on Phase-Separated Ferroelectric-Semiconductor Blends

Asadi, Kamal; de Boer, Tom G.; Blom, Paul W. M.; de Leeuw, Dago M.

Published in:
Advanced Functional Materials

DOI:
10.1002/adfm.200900383

Tunable Injection Barrier in Organic Resistive Switches Based on Phase-Separated Ferroelectric–Semiconductor Blends

By *Kamal Asadi, Tom G. de Boer, Paul W. M. Blom,* and *Dago M. de Leeuw**

This paper is dedicated to the memory of our colleague Prof. Dr. Bert de Boer who passed away January 2009.

Organic non-volatile resistive bistable diodes based on phase-separated blends of ferroelectric and semiconducting polymers are fabricated. The polarization field of the ferroelectric modulates the injection barrier at the semiconductor–electrode contact and, hence, the resistance of the comprising diodes. Comparison between the on- and off-current of the switching diodes, with the current measured for semiconductor-only diodes reveals that the switching occurs between bulk-limited, i.e., space-charge-limited, and injection-limited current transport. By deliberately varying the HOMO energy of the semiconductor and the work-function of the metal electrode, it is demonstrated that injection barriers up to 1.6 eV can be surmounted by the ferroelectric polarization yielding on/off current modulations of more than five orders of magnitude. The exponential dependence of the current modulation with a slope of 0.25 eV/decade is rationalized by the magnitude of the injection barrier.

1. Introduction

There is a growing research interest in organic memories for non-volatile data storage.[1] The majority of the literature focuses on resistive switching. The advantage of a resistive random access memory is that each element is a two-terminal device. Switching between a high- and low-resistance state is achieved by means of an appropriate electrical pulse. The state can subsequently be read out at low bias.

[*] Prof. D. M. de Leeuw, K. Asadi, T. G. de Boer, Prof. P. W. M. Blom
Zernike Institute for Advanced Materials
University of Groningen
Nijenborgh 4, 9747 AG, Groningen (The Netherlands)
E-mail: dago.de.leeuw@philips.com
Prof. D. M. de Leeuw
Philips Research Laboratories
High Tech Campus 4, 5656AE, Eindhoven (The Netherlands)
Prof. P. W. M. Blom
Holst Centre
High Tech Campus 31, 5605 KN Eindhoven (The Netherlands)

DOI: 10.1002/adfm.200900383

The memory element can be incorporated in a cross-point array where the storage medium is sandwiched between two layers of electrodes running in perpendicular directions. The rows and columns then form the word and bit lines. Using an unpatterned storage medium, a cross-point array is simple to make because it does not require strict alignment. However, for electrically symmetric switching elements application of cross-point arrays is hampered by cross talk.[2] The measured resistance equals that of the selected cell in parallel with the resistances of the memory cells in all other word and bit lines. Reliable determination of the logic value therefore requires electrical isolation of the discrete cells. The indicated solution to eliminate this cross-talk is adding a rectifying diode to each cell.[1–2] We have recently presented an integrated solution. The use of an unpatterned storage medium consisting of a phase-separated blend of an organic ferroelectric and a semiconducting polymer did yield bistable rectifying diodes.[3]

A tentative mechanism for the bistability is depicted in Figure 1. A schematic cross-section of the blend is shown in Figure 1a. Current can only flow through the unintentionally p-type doped semiconductor. For a poor injecting contact, an injection barrier exists; it is the difference between the work-function of the electrode and the highest occupied molecular orbital (HOMO) energy of the semiconductor. When the ferroelectric is poled negative, Figure 1c, the polarization charge is compensated by accumulated holes in the semiconductor. The resulting band bending effectively lowers the injection barrier. When the ferroelectric is poled positive, the polarization charge cannot be compensated by the p-type semiconductor and, therefore, is only compensated by electrons in the electrode. The injection barrier remains constant or even slightly increases.

For the design of a non-volatile two-terminal memory element, it is important to understand the origin and limit of the current modulation ratio that can be achieved. Here we address the magnitude of the injection barrier that can be surmounted by the ferroelectric polarization, and the magnitude of the current

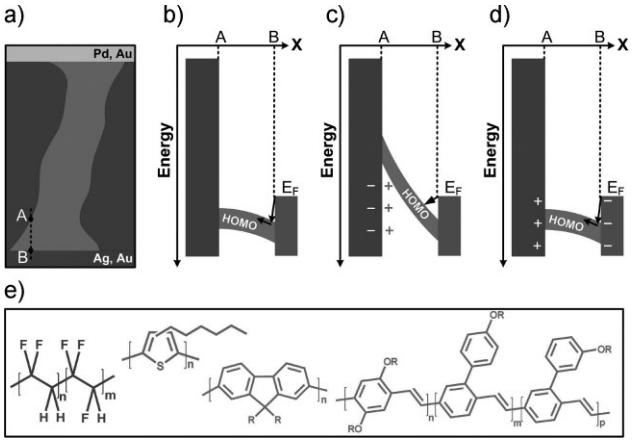

Figure 1. a) Schematic illustration of the resistive switching mechanism in diodes based on a phase-separated blend of a ferroelectric polymer (blue) and an organic semiconductor (red). a) Microstructure of the blend. b) Band diagram in the pristine, unpoled state at the interface between the metal electrode and the semiconductor phase in the blend diodes along the dashed line A–B depicted in (a). c,d) Band diagrams along the dashed line A–B when the ferroelectric is polarized both negatively and positively. e) Chemical structure of the materials used, from left to right P(VDF-TrFE), rir-P3HT, PFO and SY.

modulation that can be achieved. To that end, we deliberately varied the type of semiconductor and the work-function of the electrode. By a direct comparison between the charge transport in semiconductor-only diodes and diodes based on phase-separated blends, we demonstrate that the memory element switches from an injection-limited current to a bulk-limited current and vice versa. The resulting empirical relation between injection barrier and current modulation enables us to predict the current modulation directly from the energy levels of the materials comprising the memory element.

2. Experiments

As the ferroelectric, we used random copolymer poly(vinylidene fluoride-trifluoroethylene (P(VDF-TrFE)) (ratio 65–35). The coercive field of 50 MV m^{-1} and the remanent polarization of 0.07–0.08 C m^{-2} were derived separately from ferroelectric capacitors using a Sawyer–Tower circuit.[4] The values agree with data in the literature for a P(VDF–TrFE) (65–35) ratio.[5] As semiconducting polymers, we used commercially available polymers regio-irregular poly(3-hexylthiophene) (rir-P3HT), phenyl-substituted poly(phenylene vinylene) commercially known as super yellow (SY), and poly(9,9-dioctylfluorene) (PFO). The chemical structures of the compounds are presented in Figure 1e. The rir-P3HT was purified before use; other polymers were utilized as received.

We made two sets of diodes. First we investigated charge transport in semiconductor-only diodes. The second set comprised diodes based on blends. The semiconductor-only diodes were made by spin-coating the polymers from toluene solutions. The film thickness typically amounted to 120–200 nm. As bottom contacts, poly(3,4-ethylenedioxythiophene):polystyrene sulfonic acid (PEDOT:PSS), silver, and gold were used. We investigated charge injection from the bottom contacts. With the HOMO levels of rir-P3HT, SY and PFO amounting to 5.1, 5.4,[6] and 5.9–6.1 eV,[7,8] respectively, hole injection barriers with Ag (4.3 eV) and Au (4.8 eV) ranging from 0.3 to 1.3 eV can be obtained. It should be noted that for PFO on Ag the injection barrier of 1.8 eV suppresses the current below the leakage current due to local shorts. To prevent parasitic electron currents, a blocking palladium or gold top contact was used. In the case of PFO, the HOMO energy level of 5.9–6.1 eV prevents the formation of an Ohmic contact with PEDOT:PSS (5.1 eV) such that the bulk transport properties cannot be measured from hole-only diodes. To derive the hole transport properties of PFO, we fabricated bipolar PFO light-emitting diodes and calculated the hole current density from a theoretical fit to the current density.[9] The error in the calculated hole current density is estimated to be at most a factor of two.

For the ferroelectric–semiconductor blend diodes, the processing was optimized for 10 wt% semiconductor and 90 wt% P(VDF-TrFE). Films of about 150 nm were spin-coated from tetrahydrofuran (THF). To enhance the ferroelectricity of P(VDF-TrFE), the films were annealed in vacuum at 140 °C.[10] As bottom contacts silver and gold were used. The diodes were finished by evaporating a 70 nm top metal palladium layer through a shadow mask. The topography, as investigated with atomic force microscopy (AFM) showed a rough surface, probably due to coarse phase separation.[3] Hence, electric shorts limited the yield of functional diodes to about 80%. The current transport was measured inside a nitrogen glovebox. The top contact was grounded. Work-functions were determined inside a nitrogen glovebox using a Kelvin probe built in-house.

3. Results and Discussion

As a typical example of a semiconductor-only diode, we discuss rir-P3HT. The current density as a function of voltage is presented in Figure 2a for two different anodes, PEDOT:PSS and silver. The current density when using PEDOT:PSS is orders of magnitude larger than with silver. In the case of PEDOT:PSS, the current density scales at low bias with the voltage squared, indicating bulk-limited transport, viz. space-charge-limited current (SCLC). Observation of SCLC is expected because the work-function of PEDOT:PSS matches the HOMO energy of rir-P3HT, yielding an Ohmic contact.[11] To substantiate the lack of an injection barrier, the transport was investigated as a function of temperature as shown in Figure 2b. The transport is due to hopping, i.e., phonon-assisted tunneling. Assuming a Gaussian distribution of localized states (DOS), the transport can be modeled analytically.[12] Figure 2b shows a perfect agreement between measured and calculated current densities for all temperatures investigated. The fit constants amounted to a room temperature mobility of 6.5×10^{-7} cm^2 V^{-1} s^{-1}, which is thermally activated with an activation energy of 0.39 eV, a zero field conductivity of 1.6×10^6 S m^{-1}, and a width of the Gaussian DOS of 98 meV. The numbers agree well with reported values for P3HT.[12] The perfect fit indicates that the contact is indeed Ohmic, the injection barrier is negligible, and the current is space-charge-limited.

The current density with a silver anode is several orders of magnitude lower than the SCLC. That is expected from the difference in work-function of silver and the HOMO energy of rir-P3HT. An injection barrier of about 0.8 eV is estimated.[13] The current therefore is an injection-limited current (ILC). Due to lack of a complete transport model, the ILC transport has not been fitted

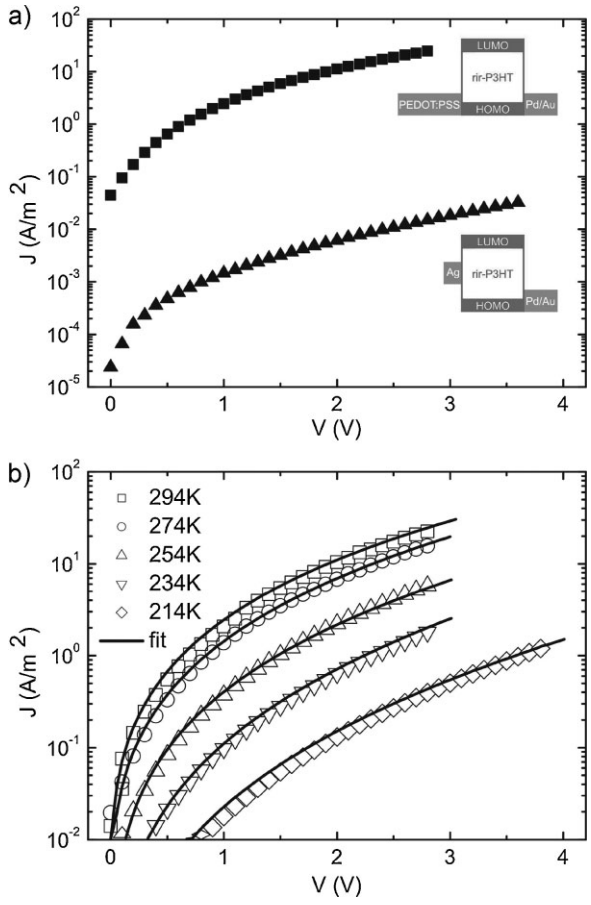

Figure 2. Current–voltage characteristics of rir-P3HT semiconductor-only diodes with PEDOT:PSS and silver anodes (a). Semiconductor layer thickness is 150 nm. PEDOT:PSS forms an Ohmic contact, and the current is space-charge-limited. The use of silver as anode results in injection-limited current. The inset shows the band diagram for the two anodes (b). Temperature dependence of the current density for diodes with PEDOT:PSS as anode (symbols). The solid line shows the calculated current density.

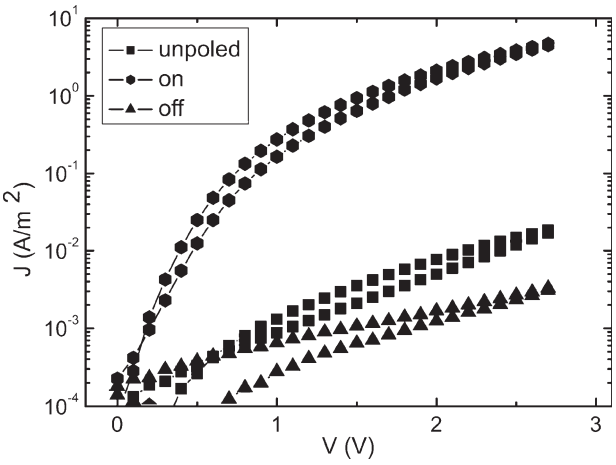

Figure 3. Current–voltage characteristics of a 10 wt% rir-P3HT, 90 wt% P(VDF-TrFE) blend diode with device area of 1 mm^2 and a film thickness of 150 nm with silver anode. The squares represent the current density in the unpoled pristine state. The hexagons and triangles represent the current density after poling the diode at −20 V and +20 V respectively.

analytically.[11] Here we will use only the phenomenological relation between barrier height and maximum current density. Semiconductor-only diodes of SY showed the same behavior. With PEDOT:PSS as anode, the current density is space-charge-limited and can be quantitatively modeled. The current density with silver or gold anodes is injection-limited.

The switching characteristics of a diode based on a *blend* of rir-P3HT and P(VDF-TrFE) with a silver anode are presented in Figure 3. In the pristine, unpoled, state the current density is low, showing that silver is a poor injecting contact. The diode can be put into a low resistance on-state and a high resistance off-state by applying 10 ms voltage pulses of −20 and +20 V, respectively. The switching occurs because the electric field at these biases exceeds the coercive field of the ferroelectric P(VDF-TrFE).[5] As explained in Figure 1, in the on-state, the negative ferroelectric polarization at the silver contact is compensated by holes in the rir-P3HT. The accumulated charges lead to band bending and, therefore, to a reduced injection barrier. In order to deduce the origin of the current modulation in the blend diodes we compare the on-current density with that of the SCLC in the rir-P3HT semiconductor-only diode and the off-current density with the ILC in the semiconductor-only diode. The normalized current densities are presented in Figure 4a. Remarkably, by using only a single normalization factor a perfect agreement for both the on- and off-current is obtained. This agreement strongly indicates that the electric current in the on-state of the blend diode is space-charge-limited, whereas the current in the off-state is injection-limited. The negatively poled silver contact therefore is Ohmic and the injection barrier can be disregarded. For further verification, the current transport in the on-state was measured as a function of temperature. The current densities were calculated with the hopping transport model using the fit parameters derived for the rir-P3HT semiconductor-only diode. Figure 4b shows that a perfect agreement for the normalized current is obtained. For the normalization, we used a factor of 3.6, slightly less than the factor of 10 as would be expected on the basis of the rir-P3HT content. One reason for this discrepancy could be the morphology. The coarse phase separation yields rough surfaces and therefore a large spread in device current densities.

Switching characteristics in diodes based on blends of P(VDF-TrFE) with a PPV derivative, SY, with silver and gold anodes, show the same qualitative behavior. Also here the current density in the off-state is injection-limited. The current density in the on-state is space-charge-limited and can be fitted analytically using exactly the same fit parameters as derived from the separate SY semiconductor-only diodes. The on/off current modulation is equal to the ratio between the SCLC and ILC. These results demonstrate that the off-current can be further suppressed by increasing the injection barrier, yielding a larger current modulation. To this end, we used PFO with a deep HOMO energy level of 5.9–6.1 eV forming an injection barrier of 1.3 eV with Au. Figure 5 shows the current–electric field (*J*–*E*) characteristic of a P(VDF-TrFE):PFO blend diode with gold electrodes. The strong suppression of the off-current leads to a current modulation exceeding five orders of magnitude below the coercive field of the ferroelectric.

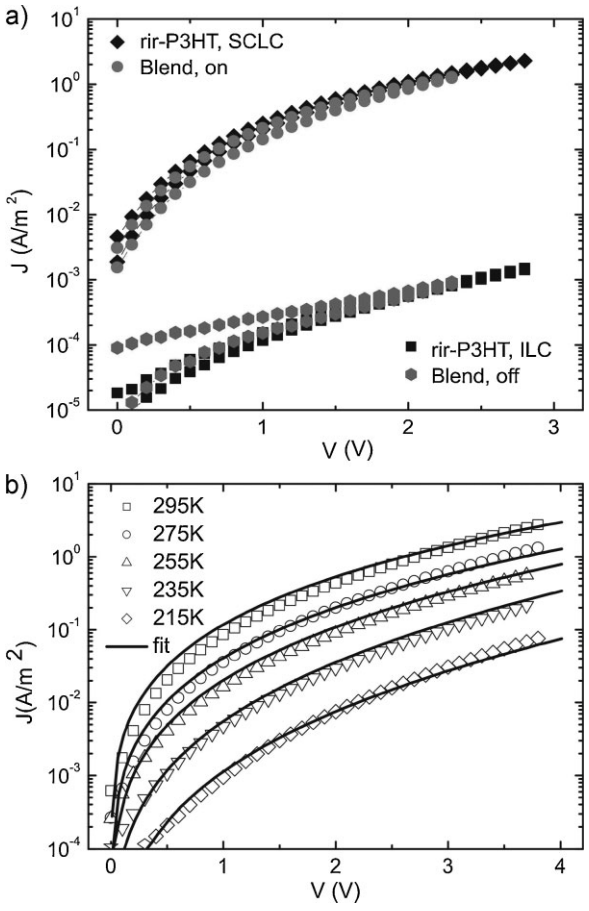

Figure 4. a) Current density as a function of voltage of a rir-P3HT semiconductor-only diode with PEDOT:PSS and silver (black) and the normalized current density of a 10 wt% rir-P3HT blend diode in the on-state (green) and the off-state (red). b) Temperature dependent current density in the 10 wt% rir-P3HT blend diode in the on-state.

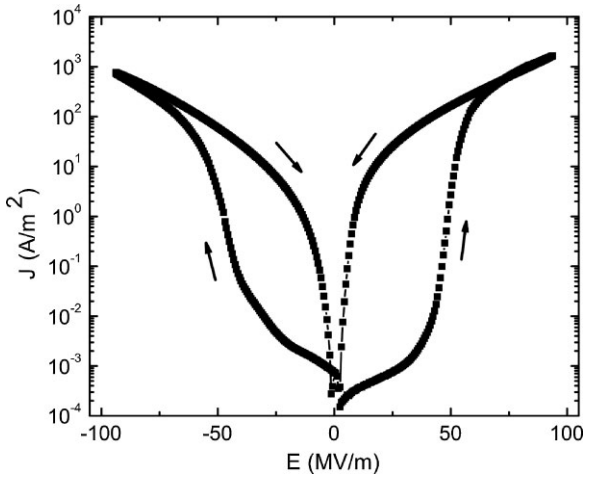

Figure 5. Current versus electric field for a blend diode comprising 10 wt% PFO and 90 wt% P(VDF–TrFE) (65–35). PFO on gold forms an injection barrier of 1.3 eV and suppresses the off-current. When the electric field exceeds the coercive field of P(VDF-TrFE), the injection barrier is modulated and leads to on/off ratio of more than five orders of magnitude measured at fields lower than the coercive field.

To estimate the maximum injection barrier that can be surmounted by the ferroelectric polarization, and to derive the maximum current modulation that can be achieved in a switching blend diode, both the work-function of the anode and the HOMO energy of the semiconductor were varied deliberately. The current modulation obtained is presented in Figure 6 on a semilogarithmic scale as a function of the injection barrier that was taken as the difference between the experimentally measured electrode work-function and the reported HOMO energy of the semiconductor.[6–8] Figure 6 shows that the current modulation increases exponentially with the injection barrier, typically a decade per 0.25 eV injection barrier, to more than five decades at a barrier of about 1.3 eV. The same functional dependence has been observed for photoprogrammable diodes.[14]

The SCLC and ILC were measured independently in semiconductor-only diodes by varying the work-function of the anode. The ratio between the SCLC and ILC current densities are presented as a function of injection barrier in Figure 6 as well. As expected the SCLC/ILC ratio as determined from discrete diodes is comparable to the on/off current ratio of switching diodes.

The current in the on-state is the maximum current that is electrostatically allowed, i.e. the SCLC. Its magnitude depends amongst others on layer thickness, hole mobility, device area and applied field. The off-state current is injection-limited. For charge injection various models have been proposed.[15] Assuming thermionic emission as the responsible injection mechanism, the current should be proportional to $\exp(-\Delta\Phi/kT)$ where $\Delta\Phi$ is the injection barrier, k is the Boltzmann constant, and T is the absolute temperature.[16] Injection models based on hopping transport yield a functional dependence for the current in the form of $\exp(-\Delta E/kT)$ where ΔE is the energy offset between the Fermi level of the metal and the energy of a certain transport level in the density of localized states.[17] This offset is proportional to the injection barrier taken as the difference between the work-function of the electrode and the HOMO energy of the semiconductor. Hence all

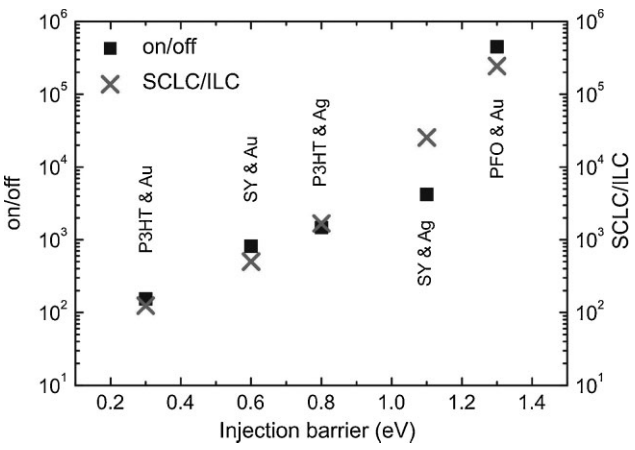

Figure 6. On/off current ratio of blend diodes (left axis), and SCLC/ILC current ratio of semiconductor-only diodes (right axis) versus injection barrier at an electric field of 20 MV m^{-1}. The injection barrier was taken as the difference between the experimentally measured work-function of the anode PEDOT:PSS, gold and silver and the reported HOMO energy level of rir-P3HT, SY, and PFO. The current modulation depends exponentially on the injection barrier, with a slope of 0.25 eV/decade.

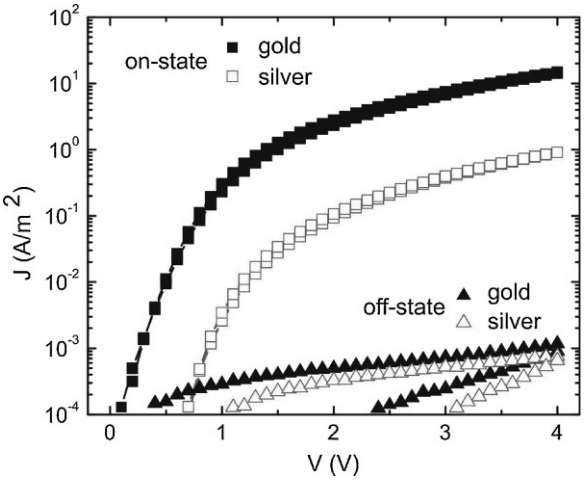

Figure 7. Comparison between the on- and off-state current of the blend diodes of 10 wt% PFO and 90 wt% P(VDF-TrFE) fabricated with different anodes; gold (filled black symbols) and silver anodes (hollow red symbols). The lower on-current, in the case of silver, demonstrates presence of an injection barrier of about 0.2 eV for PFO on silver. The off-current is limited by the leakage current of the blend diodes in both cases.

injection models predict an exponential dependence of current density on injection barrier. Since the hole mobility of the investigated semiconductors themselves are of the same order of magnitude, the width of their (Gaussian) density of localized states and the position of the transport level are comparable. As a result, the current modulation of switching diodes as well as the SCLC/ILC ratio of discrete semiconductor-only diodes exponentially depends on the injection barrier, as observed in Figure 6.

The largest hole injection barrier that we can obtain is 1.8 eV for PFO on silver. As explained in that case, the off-current is below the leakage of the diodes, meaning that the on/off ratio is not well defined. However, we still can compare the on-currents of P(VDF-TrFe):PFO diodes with gold and silver anodes, as shown in Figure 7. The on-current of diodes with silver anode is typically one order of magnitude lower than the diodes with gold anodes, meaning that the current is slightly injection-limited. Since the on/off ratio varies with 0.25 eV/decade this means that for silver in the on-state a barrier of about 0.2 eV is still present. Therefore, we estimate that the maximum barrier that can be switched by the ferroelectric polarization is 1.6 eV. From Figure 6, such a barrier modulation is expected to lead to a maximum achievable current modulation of 6–7 decades. Taking into account that the number of bits in a cross-point memory array is proportional to the current modulation squared, a promising future in low-end data storage applications is expected.

4. Conclusion

In conclusion, the current transport in bistable organic resistive diodes based on phase-separated blends of ferroelectric and semiconducting polymers has been investigated. The diodes switch between bulk-limited (space-charge-limited), and injection-limited transport. The current modulation depends exponentially on the injection barrier, with a slope of 0.25 eV/decade. Barriers up to 1.6 eV can be surmounted by the ferroelectric polarization, yielding current modulations up to five orders of magnitude or more.

5. Experimental

The ferroelectric polymer (P(VDF–TrFE) (65–35)) was purchased from Solvay and used without further purification. P(VDF–TrFE) dissolved in THF. Silver electrodes (40 nm) were evaporated via shadow masks onto clean glass substrates with 1 nm of chromium acting as adhesion layer. The P(VDF-TrFE) solution was then spin-coated onto the substrate. Following an annealing step in vacuum oven at 140 °C, the capacitors were completed with the evaporation of the silver top contact, and they were characterized using a Sawyer–Tower circuit. We purified rir-P3HT (Rieke Metals) by dissolving it in distilled toluene, dedoping it with hydrazine, and precipitating it in methanol. The fraction collected was Soxhlet-extracted with methanol, *n*-hexane, and dichloromethane until the extraction solvent was colorless. The dichloromethane fraction was precipitated in methanol, collected, dissolved in chloroform and precipitated again in methanol. The collected fraction was dried under vacuum and stored in the glovebox under a nitrogen atmosphere. SY (Covion (Merck)) and PFO (TNO) were both used as received. To fabricate the semiconductor-only diodes, we spin-coated PEDOT (H. G. Starck) on glass substrates with prepatterned ITO contacts. Semiconductor materials were dissolved in toluene and filtered with 5 μm polytetrafluorethylene (PTFE) filters. Subsequently the filtered solution was spin-coated onto the substrates to form a film with thickness in the range of 120–200 nm. Palladium (20 nm) gold (70 nm) top contacts were deposited via shadow mask. In the case of PFO, we deposited barium (5 nm) and aluminum (100 nm). For the ferroelectric–semiconductor blend diodes, we evaporated gold (40 nm) or silver (40 nm) on clean glass substrates with an adhesion layer of chromium (1 nm). We optimized the processing for 10 wt% semiconductor and 90 wt% P(VDF-TrFE). Materials were codissolved in THF. Films of about 150 nm were formed via spincoating after filtration of the solution with 1 μm PTFE filters. Following an annealing step at 140 °C in vacuum, the diodes were completed by the evaporation of the palladium top contact (70 nm) through a shadow mask. All electrical measurements were carried out in a nitrogen-filled glovebox with a Keithley 2400 source meter. Work-functions were determined inside a nitrogen glovebox using a Kelvin probe that was built in-house. AFM (NanoScope IV-Veeco Instruments) measurements were carried out in an ambient atmosphere.

Acknowledgements

Zernike Institute for Advanced Materials financially supported this study. We thank TNO for supplying samples of PFO. M. Kuik and H. T. Nicolai are gratefully acknowledged for modeling advice and J. Harkema for technical assistance.

Received: March 6, 2009
Revised: June 5, 2009
Published online: August 26, 2009

[1] J. C. Scott, L. D. Bozano, *Adv. Mater.* **2007**, *19*, 1451.
[2] J. C. Scott, *Science* **2004**, *304*, 62.
[3] K. Asadi, D. M. de Leeuw, B. de Boer, P. W. M. Blom, *Nat. Mater.* **2008**, *7*, 547.
[4] C. B. Sawyer, C. H. Tower, *Phys. Rev.* **1930**, *35*, 269.
[5] T. Furukawa, *Phase Transitions* **1989**, *18*, 143.
[6] L. L. Chua, J. Zaumseil, E. C. W. Ou, P. K. H. Ho, H. Sirringhaus, R. H. Friend, *Nature* **2005**, *434*, 194.
[7] A. J. Campbell, D. D. C. Bradley, H. Atoniadis, *J. Appl. Phys.* **2001**, *89*, 3343.

[8] L. S. Liao, C. S. Lee, S. T. Lee, M. Inbasekaran, W. W. Wu, in *Conjugated Polymers and Molecular Interfaces*, (Eds: W. R. Salaneck, K. Seki, A. Kahn, J.-J. Pireaux), Marcel Dekker, New York **2002**.
[9] T. van Woudenbergh, J. Wildeman, P. W. M. Blom, J. J. A. M. Bastiaansen, B. M. W. Langeveld-Voss, *Adv. Funct. Mater.* **2004**, *14*, 677.
[10] H. Kodama, Y. Takahashi, T. Furukawa, *Ferroelectrics* **1997**, *203*, 433.
[11] Y. Shen, A. R. Hosseini, M. H. Wong, G. G. Malliaras, *ChemPhysChem* **2004**, *5*, 16.
[12] C. Tanase, E. J. Meijer, P. W. M. Blom, *Phys. Rev. Lett.* **2003**, *91*, 216601.
[13] J. K. J. Van Duren, V. D. Mihailetschi, P. W. M. Blom, T. van Woudenbergh, J. C. Hummelen, M. T. Rispens, R. A. J. Janssen, M. M. Wienk, *J. Appl. Phys.* **2003**, *94*, 4477.
[14] P. Zacharias, M. C. Gather, A. Kohnen, N. Rehmann, K. Meerholz, *Angew. Chem. Int. Ed.* **2009**, *48*, 4038.
[15] D. Braun, *J. Polym. Sci. Part B* **2003**, *41*, 2622.
[16] J. C. Scott, G. G. Malliaras, *Chem. Phys. Lett.* **1999**, *229*, 115.
[17] V. I. Arkhipov, E. V. Emelianova, Y. H. Tak, H. Bassler, *J. Appl. Phys.* **1998**, *84*, 848.